EAI Endorsed Transactions
on e-Learning

Research Article EAI.EU

Tea category classification via 5-layer customized convolutional neural network

Xiang Li[1], Mengyao Zhai[2] and Junding Sun[1,*]

[1]College of Computer Science and Technology, Henan Polytechnic University, Jiaozuo, Henan 454000, P R China
[2]College of Humanities and Education, Hebi Polytechnic, Hebi, Henan, 458030, P R China

Abstract:

INTRODUCTION: Green tea, oolong, and black tea are the three most popular teas in the world. If classified tea by manual, it will not only take a lot of time, but also be affected by other factors, such as smell, vision, emotion, etc.
OBJECTIVES: Other methods of tea category classification have the shortcomings of low classification accuracy, weak robustness. To solve the above problems, we proposed a method of deep learning.
METHODS: This paper proposed a 5-layer customized convolutional neural network for 3 tea categories classification.
RESULTS: The experimental results show that the method has fast speed and high accuracy of tea classification, which is 97.96%.
CONCLUSION: Compared with state-of-the-art methods, our method has better performance than six state-of-the-art methods.

Keywords: convolutional neural network, customized convolution neural network, deep learning, tea category classification.

Received on 10 March 2021, accepted on 30 April 2021, published on 05 May 2021

doi: 10.4108/eai.5-5-2021.169811

*Junding Sun. Email: sunjd@hpu.edu.cn

1. Introduction

Tea can promote digestion, inhibit arteriosclerosis, reduce the incidence of cardiovascular and cerebrovascular diseases [1]. Therefore, more and more people have begun to insist on drinking tea every day. According to the different kinds of tea plants and the different tea production ways, tea can be divided into six categories: green tea, black tea, oolong, white tea, black tea and yellow tea. Among them, green tea [2], oolong [3], and black tea [4] are the three most popular teas in the world . If we classified tea by manual, it will not only take a lot of time, but also be affected by other factors, such as smell, vision, emotion, etc. These factors increase the uncertainty of the classification results.

In recent years, many scholars try to use computer vision technology to classify tea. Jian, et al. [5] presented a genetic neural network (GNN) to identify tea leaves. Yu, et al. [6] employed least-square support vector machine (LSSVM). Zhang, et al. [7] proposed a twelve-layer deep convolutional neural network with stochastic pooling for tea category classification. The experiment results show that the method gives a good result. Especially, the overall accuracy (OA) of three-tea categories is 98.33%. Lin, et al. [8] proposed a method that used 14 tea image features to recognition and classification the categories of tea. This method described a new automated classification method for Wuyi rock tealeaves based on the best penalty parameter selection for the support vector machine with Radial Basis Function kernel. The experiment results show that this method recognition rate of fresh tealeaves is 91.00%. Yang [9] proposed to use fuzzy support vector machine (FSVM) to classify tea leaves. Ren, et al. [10] used near-infrared (NIR) technology to assess black tea tenderness and rankings. They proposed a multi-variable selection strategy based on the variable space optimization from big to small. The experiment results show that the model with a radial basis function achieves the best predictive results with the correct discriminant rate of 95.28% in this paper. Wu [11] presented a weighted k-nearest neighbors (WKNN) algorithm for tea category identification via a 3-CCD optical camera. Cattani and Rao [12] used Jaya algorithm to identify tea categories. Liu [13] used generalized eigenvalue proximal support vector machine (GEPSVM) for tea category identification. Chen and Chen [14] employed gray-level occurrence matrix (GLCM) to identify five categories of tea leaves.

Through the analysis of the methods in the above literature to know, these methods have some shortcomings, such as complex network structure, weakness robustness, redundant operation of feature extraction. To solve the first problem, we proposed a model with a sample network structure. And to achieve fast and accurate tea classification, this paper proposed a 5-layer customized convolution neural network for tea classification of green tea, oolong tea and black tea. The experiment results of 10-fold cross validation show that our model has better robustness and better performance than state-of-the-art methods.

The structure of this paper is as follows: Section 2, introduced our dataset of experiments, and we described the characteristics of each tea category. Section 3, introduced the structure of our proposed model and the functions of each network component. It also explained the measures used in the experiments. Section 4, showed the results of experiments, and compared our method with state-of-the-art methods. Section 5, concluded this paper and pointed out the direction of our future study.

2. Dataset

The dataset of this paper consists of three-tea categories: Green tea, Oolong, and black tea. Each category has 300 images. All categories have 900 images in all. As shown in Figure 1, the shape of green tea is long and thin, the color is green mixed with yellow, and the strips are slightly curved. Oolong is a compact round shape, which is green mixed with black. And for black tea, the leaves are thicker and the color is dark brown.

(a) Green tea (b) Oolong (c) Black tea

Figure 1. Samples of our dataset

3. Methodology

In this section, we will introduce the method of our study. We used the convolutional neural network to classify tea categories. To easily understand this paper. Table 15 shows all variables used in our study. Table 16 gives the abbreviation and their full names. Table 15 and Table 16 are in the appendix at the end of the paper.

3.1. Convolution

Convolution is the result of two variables multiplied together in a range [15]. In our method, we used convolution operation to extract the features of input information [16]. The information in receptive field of convolution kernel calculated by convolution operators to obtain the extracted features. Through the receptive field of convolution kernel scanning the information matrix continuously and performs the convolution operation constantly [17-19]. All the extracted features are obtained. Figure 2 shows a convolution operation of the convolution kernel performing the feature extraction.

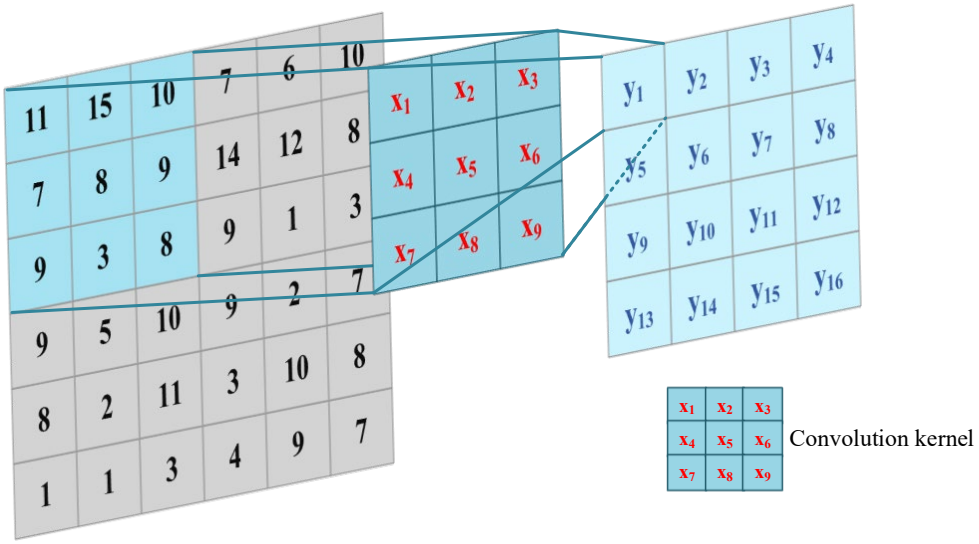

Figure 2. Convolution operation

Here, x_1 to x_9 are convolution operators. And y_1 to y_{16} are the obtained features by convolution operation. The output size calculation method of convolution operation is as follows.

$$O_c = \left\lfloor \frac{I_c + 2P - X}{R_c} + 1 \right\rfloor \quad (1)$$

Here, O_c represents the output size of convolution operation [20]. I_c represents input information size of convolution operation. P represents the size of padding. X represents the size of convolution kernel. And R_c represents the stride size of convolution kernel. Through the use of convolutional layers, the effective extraction of image features can be achieved, and it also has the characteristics of parameter sharing and sparse connection.

3.2. Convolutional operation in Convolutional Neural Network

Figure 3 shows how the convolution kernel performs the convolutional operation in convolutional neural network. As shown in Figure 3, "Input" represents the input information of convolutional neural network (CNN). "Kernel" represents the convolution kernel. "Conv-in-Run" represents the process of convolutional operation [21]. "Conv" represents the convolutional layer. "Stack" represents consecutive convolutional layers. "Output" represents the output feature of the model. Here, the input information was scanned by convolution kernel [22]. The convolution kernel operator performs convolutional operation. The specific process is: each convolution kernel operator multiplies the corresponding input information to get the output. And the output of a convolution kernel is the sum of the outputs of all convolution kernel operators. CNN uses this network structure to quickly capture the features of input information.

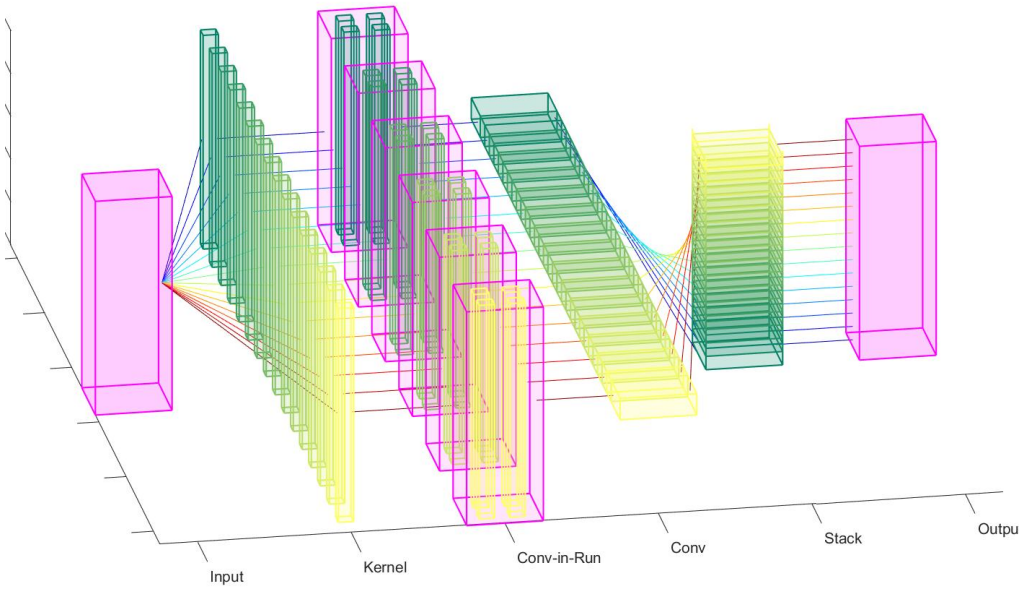

Figure 3. Convolutional operation in convolutional neural network

Equation (2) and (3) show the output calculate method of neurons.

$$O_n = \sum_{a=1}^{m} w_a x_a + b_a \quad (2)$$

$$O_\sigma = \sigma(O_n) \quad (3)$$

Here, O_n represents the output of a neuron without activation function. m represents the number of neurons in the previous layer connected to it. a represents the index of neurons it starts from 1. w_a represents the weight of a-th neuron. x_a represents the input of a-th neuron. b_a represents the bias of a-th neuron. O_σ represents the output of a neuron with activation function. And σ represents the activation function [23].

3.3. Pooling

The function of pooling is to reduce the feature dimensions, prevent overfitting and enhance the robustness of the model [24]. There are two common pooling – max-pooling and average pooling [25]. The difference between the two methods is that the output value of max-pooling is the maximum number of the receptive field of pooling kernel

[26], and the output value of average pooling is the average number of all the numbers in the receptive field of pooling kernel. Figure 4 shows the two common methods of pooling.

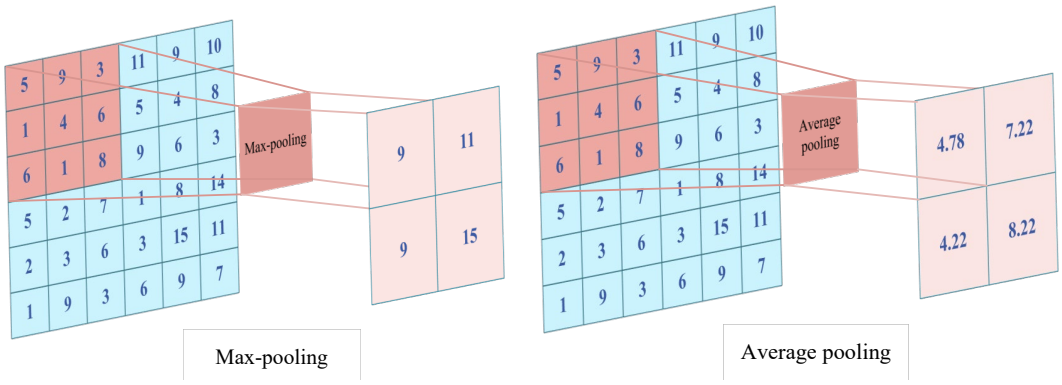

Figure 4. Max-pooling and average pooling

The output size calculation method of pooling is as follows.

$$O_p = \left\lceil \frac{I_p - D}{R_p} + 1 \right\rceil \quad (4)$$

Here, O_p represents the output size of pooling operation. I_p represents the input size of pooling operation. D represents the size of pooling kernel. R_p represents the stride size of pooling kernel. The pooling layer can better implement dimensionality reduction operations and reduce overfitting.

3.4. Batch Normalization

Batch normalization (BN) works to speed up model training [27], improve the generalization ability of the network and improve model accuracy by disordering the sequence of training data. The calculation process of BN is as follows [28]. First, calculate the mean of mini-batch data. Second, calculate the variance of mini-batch data. Third, normalize the mini-batch data. Finally, output the data that perform the scale and shift on the data obtained by the above operations [29]. Formula (5) to (8) show the output calculated methods of BN.

$$M_j = \frac{1}{n}\sum_{i=1}^{n} Q_i \quad (5)$$

$$V_j^2 = \frac{1}{n}\sum_{i=1}^{n}(Q_i - M_j)^2 \quad (6)$$

$$\hat{Q}_i = \frac{Q_i - M_j}{\sqrt{V_j^2 + \gamma}} \quad (7)$$

$$BN_{\alpha,\beta}(Q_i) = \alpha \cdot \hat{Q}_i + \beta \quad (8)$$

Here, Q_i represents the ith data in the jth mini-batch. i represents the index of data in the j th mini-batch. n represents the number of j th mini-batch data. M_j represents the mean value of j th mini-batch data. V_j^2 represents the variance of j th mini-batch data. γ is a constant, which aims to avoid invalid calculation when the V_j^2 is 0. $\hat{Q}_i$ represents the output of normalization. α and β represent the parameters to be learned in BN. $BN_{\alpha,\beta}(Q_i)$ represents the output of BN when the input data is Q_i.

3.5. Rectified Linear Unit

Rectified Linear Unit (ReLU) is a common activation function in convolutional neural network. Which works to alleviate the gradient disappearance and improve the training speed of the model [30]. The ReLU curve is shown in Figure 5. When $x > 0$, the value of y is equal to the value of x. When $x \leq 0$, the value of y is equal to 0. And the output calculate method of ReLU is followed by (9).

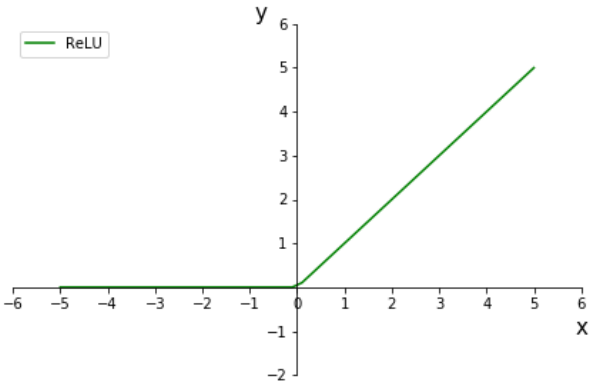

Figure 5. Rectified Linear Unit curve

$$O_R = \begin{cases} w^T z + b, z > 0 \\ 0, z \leq 0 \end{cases} \quad (9)$$

Here, z represents the input of ReLU. O_R represents the output of ReLU. w^T represents the weight transpose matrix of neural. And b represents the bias of a neural [31]. After ReLU calculated, the features with positive input can be output normally, while the features with negative input will be filtered out [32]. Therefore, ReLU can effectively improve the learning speed of model parameters in back propagation [33].

3.6. Structure of customized CNN

The structure of our model is made up of three convolutional layers, and two fully connected layers. Figure 6 shows the structure more vividly. After each convolutional layer, BN and ReLu are followed. Table 1 shows the value settings of hyperparameters in our model.

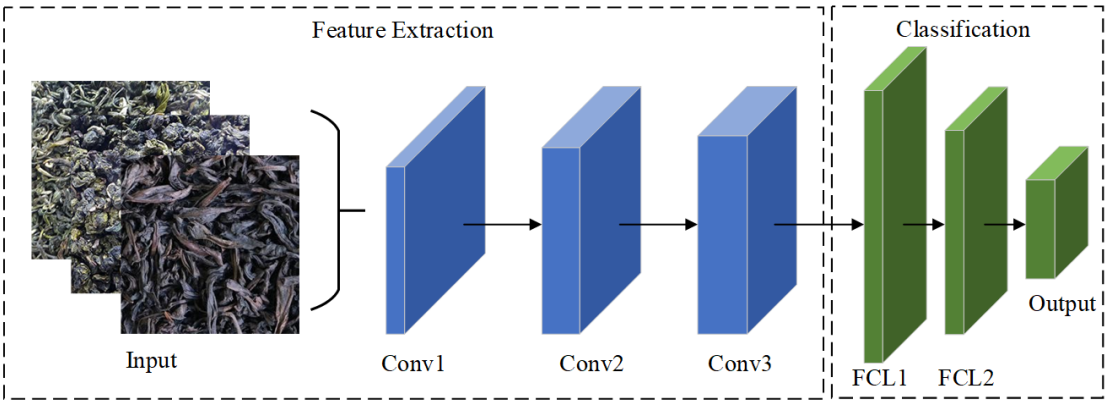

Figure 6. The structure of our model

Table 1. The values of hyperparameters of our model

Layer	Input	Conv1	Conv2	Conv3	FCL1	FCL2

Weights		8 3x3 /2	16 3x3 /2	32 3x3 /2	32768x2048	2048x3
Size	256x256	128x128x8	64x64x16	32x32x32	2048	3

Here, Conv represents the convolutional layer. FCL represents the fully-connected layer. The input size of our model is 256*256. All convolution kernel size is 3*3, and all convolution kernel stride size is 2. The input channels of the first convolutional layer are 8, output channels of that are 16. The input channels of the second convolutional layer are 16, output channels of that are 32. And the number of neurons in FCL and the output size of each layer in our model as shown in Table 1.

3.7. Measures

In order to better present the detection performance of our model, the confusion matrix is introduced as shown in Table 2. Here, TP represents the actual class is positive and the predicted class is positive too. FP represents the actual class is negative but the predicted class is positive [34]. FN represents the actual class is positive but the predicted class is negative. And the TN represents the actual class is negative and the predicted class is negative too. Besides, we defined five confusion matrix metrics: Sensitivity, Specificity, Precision, F1 and Micro-averaged F1 (MF1). The respective calculation methods are as follows.

Table 2. Confusion Matrix.

Confusion Matrix		Actual Class	
		Positive	Negative
Predicted Class	Positive	TP	FP
	Negative	FN	TN

$$\text{Sensitivity} = \frac{TP}{TP+FN} \tag{10}$$

$$\text{Specificity} = \frac{TN}{TN+FP} \tag{11}$$

$$\text{Precision} = \frac{TP}{TP+FP} \tag{12}$$

$$\text{F1} = \frac{2*Sensitivity*Precision}{Sensitivity+Precision} \tag{13}$$

$$\text{Sensitivity}_{micro} = \frac{\sum_{c=1}^{d} TP_i}{\sum_{c=1}^{d} TP_i+\sum_{c=1}^{d} FN_i} \tag{14}$$

$$\text{Precision}_{micro} = \frac{\sum_{c=1}^{d} TP_i}{\sum_{c=1}^{d} TP_i+\sum_{c=1}^{d} FP_i} \tag{15}$$

$$\text{MF1} = \frac{2*\text{Sensitivity}_{micro}*\text{Precision}_{micro}}{\text{Sensitivity}_{micro}+\text{Precision}_{micro}} \tag{16}$$

Equation (14) and (15) show the calculation methods of $\text{Sensitivity}_{micro}$ and Precision_{micro}. Here, c represents the index of categories, it starts from 1. d represents the number of categories.

3.8. Cross Validation

To better test the robustness of our model, the 10-fold cross validation is also introduced. We divide the dataset into 10 equal subsets and number them, select the number 1 as the test set, and the other subsets as the training set [35]. Take turns, till to select the number 10 as the test set, and the other subsets as the training set. Put these new datasets into the experiment [36], and record the experimental results. After obtaining the results of all experiments, the average value is calculated, and which is the result of 10-fold cross validation [37].

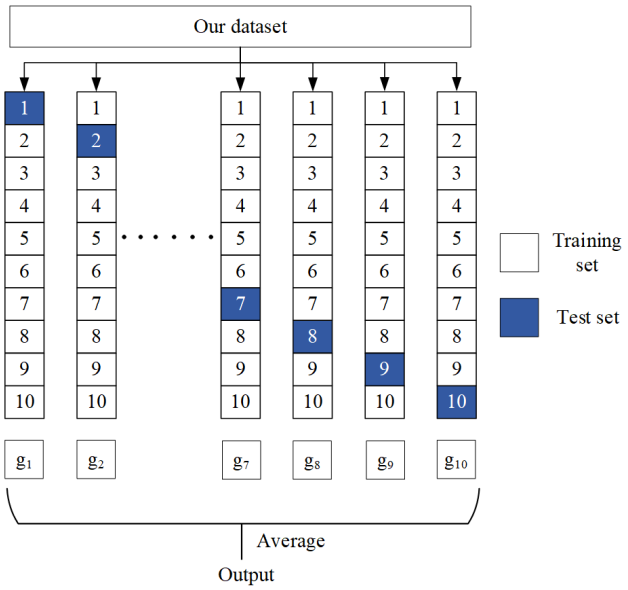

Figure 7. 10-fold cross validation.

And we performed 10 runs of 10-fold cross validation in the following experiments. An ideal 10-fold cross validation confusion matrix and an ideal 10 runs of 10-fold cross validation confusion matrix are as shown in Table 3.

Table 3 Two ideal confusion matrix.

Confusion Matrix		Actual Class (10-fold cross validation)			Actual Class (10 runs of 10-fold cross validation)		
		Green tea	Oolong	Black tea	Green tea	Oolong	Black tea
Predicted Class	Green tea	300	0	0	3000	0	0
	Oolong	0	300	0	0	3000	0
	Black tea	0	0	300	0	0	3000

4. Experiment Result and Discussions

4.1 Statistical Analysis

In this part, we showed the confusion matrix of our method and the five metrics of confusion matrix. All data as shown in Table 4 and Table 5.

Table 4. 10 runs of 10-fold cross validation

Confusion Matrix	Actual Class (10-fold cross validation)		
	Green tea	Oolong	Black tea
Predicted Class — Green tea	2956	19	25
Predicted Class — Oolong	33	2919	48
Predicted Class — Black tea	41	18	2941

Table 5. Five metrics of confusion matrix (unit: %)

	Sensitivity	Specificity	Precision	F1
Green tea	98.53	98.77	97.56	98.04
Oolong	97.30	99.38	98.75	98.02
Black tea	98.03	98.78	97.58	97.81
Micro-averaged				97.96

Table 5 shows the F1 results of green tea and oolong are beyond micro-averaged F1, and even though the black tea has achieved good results in specificity and precision, its overall performance is not as good as other teas. We believe that the reason for this result is green tea and oolong have more obvious characteristic information than black tea. Because the black tea is relatively large and the color is darker than others, it is difficult for the model to detect the characteristics of black tea.

4.2 Optimal number of Convolutional layers

In order to prove the rationality of our proposed model structure, we conducted an ablation study. We set the number of convolutional layers to 2 and 4, and observe what will happen to the results. Here, Table 5 and Table 6 show the confusion matrix results of our model has two convolutional layers. Table 7 and Table 8 show the confusion matrix results of our model has four convolutional layers.

Compare Table 7 with Table 5, all results of metrics in Table 7 have shown a clear downward trend. We believe the reason for this is that three convolutional layers structure have more powerful detection than two convolutional layers structure. Therefore, the performance of each metric in Table 5 is better than Table 7.

Table 6. Confusion matrix of two convolutional layers

Confusion Matrix		Actual Class (10-fold cross validation)		
		Green tea	Oolong	Black tea
Predicted Class	Green tea	2943	24	33
	Oolong	39	2916	45
	Black tea	44	37	2919

Table 7. Five metrics of two convolutional layers (unit: %)

	Sensitivity	Specificity	Precision	F1
Green tea	98.1	98.62	97.26	97.68
Oolong	97.2	98.98	97.95	97.57
Black tea	97.3	98.7	97.4	97.35
Micro-averaged				97.53

Table 8. Confusion matrix of four convolutional layers

Confusion Matrix		Actual Class (10-fold cross validation)		
		Green tea	Oolong	Black tea
Predicted Class	Green tea	2924	34	42
	Oolong	28	2941	31
	Black tea	34	46	2920

Table 9. Five metrics of four convolutional layers (unit: %)

	Sensitivity	Specificity	Precision	F1
Green tea	97.47	98.97	97.92	97.69
Oolong	98.03	98.67	97.35	97.69
Black tea	97.33	98.78	97.56	97.45
Micro-averaged				97.61

Compare Table 9 with Table 5, all results of metrics in Table 9 have shown a clear downward trend too. But the performance of each metric in Table 9 is better than Table 7. Here, due to the overfitting of the four convolutional layers structure, the performance of which is not beyond the three convolutional layers structure. The impact of overfitting on model detection performance is more serious than the limitation of the two convolutional layer network structure on model performance. Concluded, under the condition of keeping the same values of other parameters in the model, has three convolutional layers structure get the best detection performance for tea category. This also proves the rationality of the model structure of our proposed. Figure 8 shows this conclusion more vividly than other tables. Here, Sen represents sensitivity. Spe represents specificity. Pre represents precision.

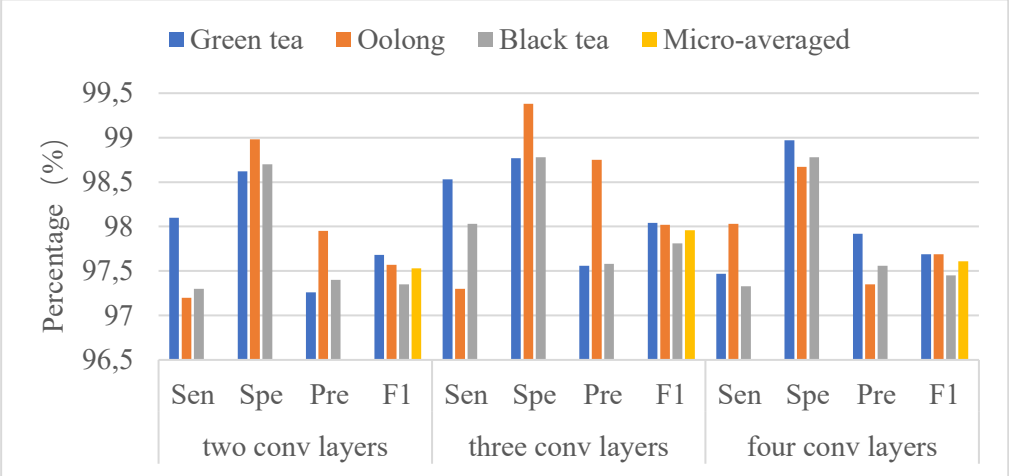

Figure 8. Performance of different number of convolutional layers

4.3 Optimal of fully-connected layers

In this part, we compared with the results of different number of fully-connected layers. Table 10 and Table 11 show the data of 1 fully-connected layer. Table 12 and Table 13 show the data of 3 fully connected layers.

Table 10. Confusion matrix of 1 FCL

Confusion Matrix		Actual Class (10-fold cross validation)		
		Green tea	Oolong	Black tea
Predicted Class	Green tea	2926	33	41
	Oolong	62	2893	45
	Black tea	24	32	2944

Table 11. Five metrics of 1 FCL (unit: %)

	Sensitivity	Specificity	Precision	F1
Green tea	97.53	98.57	97.14	97.34
Oolong	96.43	98.92	97.8	97.11
Black tea	98.13	98.57	97.16	97.65
Micro-averaged				97.37

Here, we show the results of the model that has three convolutional layers and 1 fully-connected layer. Compare Table 11 with Table 5, the MF1 of Table 11 is 97.37%, which is 0.59% lower than Table 5. It proves the performance of our model (2 fully-connected) is better than the model which has 1 fully-connected layer. This shows that the model with 1 fully-connected layer cannot be applied to tea category classification well.

Table 12. Confusion matrix of 3 FCL

Confusion Matrix		Actual Class (10-fold cross validation)		
		Green tea	Oolong	Black tea
Predicted Class	Green tea	2897	55	48
	Oolong	41	2896	63
	Black tea	45	33	2922

Table 13. Five metrics of 3 FCL (unit: %)

	Sensitivity	Specificity	Precision	F1
Green tea	96.57	98.57	97.12	96.84
Oolong	96.53	98.53	97.05	96.79
Black tea	97.4	98.15	96.34	96.87
Micro-averaged				96.83

Here, we show the results of the model that has three convolutional layers and 3 fully-connected layers. Compare Table 13 with Table 5, the MF1 of Table 13 is 96.83%, which is 1.13% lower than Table 5. And it is also 0.54% lower than Table 11. It proves the performance of the model with 3 fully-connected layers is the worst. We believe that the cause of this result is overfitting. The model with 3 fully-connected layers has overfitting, which leads to a decrease in performance. From the above content, it can be seen that in the feature extraction part and the classification part, overfitting could cause a greater negative impact on model performance. Figure 9 shows this conclusion more vividly than other tables. Here, Sen represents sensitivity. Spe represents specificity. Pre represents precision.

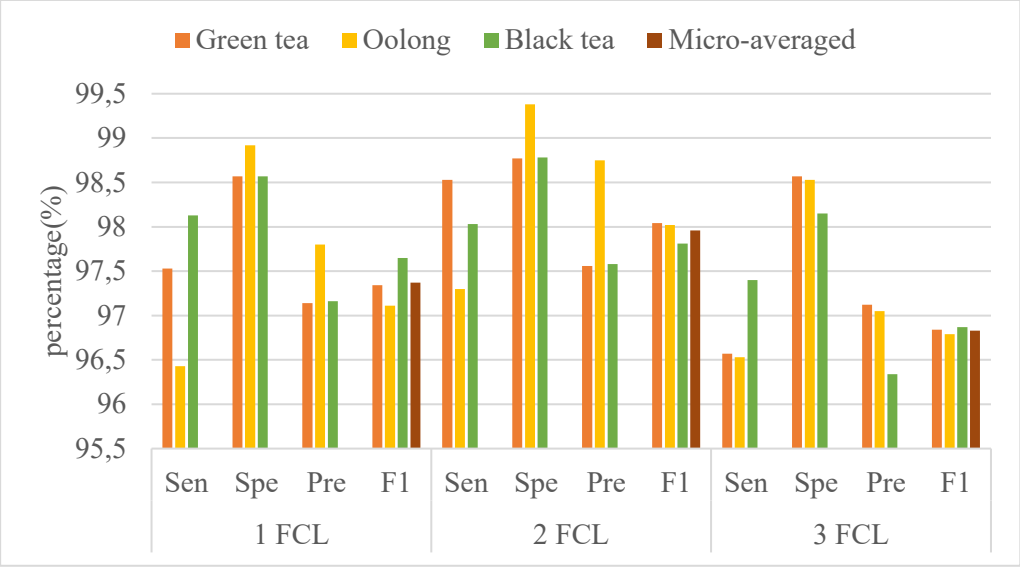

Figure 9. Performance of different number of fully-connected layers

4.4 Comparison with State-of-the-art Approaches

All the algorithms were run via 10 runs of 10-fold cross validation on our dataset. The MF1 results as shown is Table 14. Here, we compared our method with six state-of-the-art methods.

Table 14. Compare with the state-of-the-art methods (unit: %)

Methods	MF1

GNN [5]	95.10
FSVM [9]	96.08
WKNN [11]	93.46
Jaya [12]	97.30

GEPSVM [13]	97.12
GLCM [14]	86.12
Ours	97.96

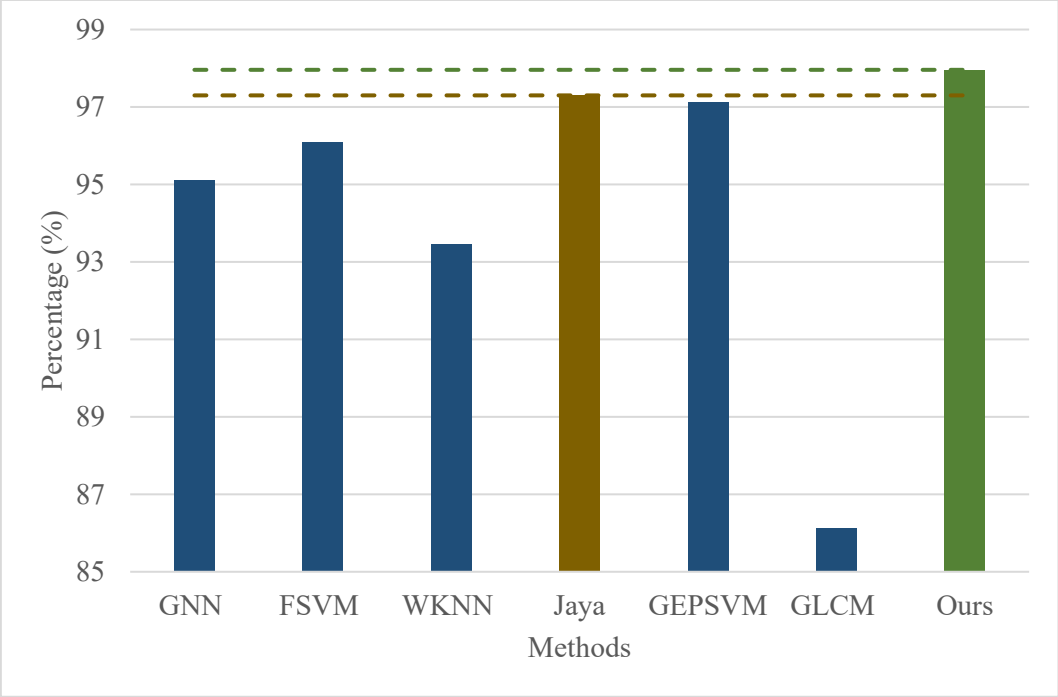

Figure 10. Compared with all methods

As shown in Table 14, the MF1 of our method is 97.96%. The Jaya methods obtained the best performance in state-of-the-art methods, which is 97.30%. As an obvious contrast, MF1 of our method is 0.66% higher than that of Jaya. Figure 10 shows this point more vividly. The brown histogram is Jaya method and the green histogram is our method. The distance between the brown dotted line and the green dotted line reflects the superiority of our algorithm. Therefore, Table 14 proves the effectiveness of our proposed method.

5 Conclusion

In this paper, we proposed the method of using a 5-layer customized convolutional neural network to perform tea category classification. The results of the experiment show our method obtained better performance than the state-of-the-art methods on MF1.

In future studies, we will continue working on computer vision and designing convolutional neural networks for solving more complex classification problems. Meanwhile, we also try to use swarm intelligence optimization algorithms to optimize the values of hyperparameters in the network. Some advanced CNN techniques [38], such as advanced pooling [39] and attention neural network [40], will be tested.

Appendix

Table 15. Variable definition table

Variable Name	Variable Meaning
a	Index of neurons it starts from 1.
$BN_{\alpha,\beta}(Q_i)$	Output of BN when the input data is Q_i.
b	Bias of a neural.
b_a	Bias of a-th neuron.
c	Index of categories, it starts from 1.
D	Size of pooling kernel.
d	Number of categories.
X	Size of convolution kernel.
x_1	Convolution operator.
x_9	Convolution operator.
x_a	Input of a-th neuron.
y_1	Obtained features by convolution operation.
y_{16}	Obtained features by convolution operation.
I_c	Input information size of convolution operation.
I_p	Input size of pooling operation.
i	Index of data in the jth mini-batch.
M_j	Mean value of jth mini-batch data.
m	Number of neurons in the previous layer connected to it.
n	Number of jth mini-batch data.
O_c	Output size of convolution operation.
O_n	Output of a neuron without activation function.
O_p	Output size of pooling operation.
O_σ	Output of a neuron with activation function.
P	Size of padding.
Q_i	ith data in the jth mini-batch.
$\hat{Q}_i$	Output of normalization.
O_R	Output of ReLU.
R_c	Stride size of convolution kernel.
R_p	Stride size of pooling kernel.
V_j^2	Variance of jth mini-batch data.
w_a	Weight of a-th neuron.
w^T	Weight transpose matrix of neural.
z	Input of ReLU.
α	A parameter to be learned in BN.
β	A parameter to be learned in BN.
γ	A constant, which aims to avoid invalid calculation when the V_j^2 is 0.

σ	Activation function.

Table 16. Abbreviation table

Abbreviation	Full Definition
BN	Batch Normalization.
CNN	Convolutional Neural Network.
Conv	Convolutional Layer.
FCL	Fully-Connected Layer.
FN	False Negative.
FP	False Positive.
FSVM	Fuzzy Support Vector Machine.
GEPSVM	Generalized Eigenvalue Proximal Support Vector Machine.
GLCM	Gray-Level Occurrence Matrix.
GNN	Genetic Neural Network.
NIR	Near-Infrared.
LSSVM	Least-Square Support Vector Machine.
MF1	Micro-Averaged F1.
OA	Overall accuracy.
Pre	Precision.
ReLU	Rectified Linear Unit.
Sen	Sensitivity.
Spe	Specificity.
TN	True Negative.
TP	True Positive.
WKNN	Weighted K-Nearest Neighbors.

References

[1] Y. Katanasaka *et al.*, "Kosen-cha, a Polymerized Catechin-Rich Green Tea, as a Potential Functional Beverage for the Reduction of Body Weight and Cardiovascular Risk Factors: A Pilot Study in Obese Patients," (in English), *Biol. Pharm. Bull.,* Article vol. 43, no. 4, pp. 675-681, Apr 2020, doi: 10.1248/bpb.b19-00921.

[2] D. L. Meneses, Y. Ruiz, E. Hernandez, and F. L. Moreno, "Multi-stage block freeze-concentration of green tea (Camellia sinensis) extract," (in English), *Journal of Food Engineering,* Article vol. 293, p. 7, Mar 2021, Art no. 110381, doi: 10.1016/j.jfoodeng.2020.110381.

[3] W. Tanticharakunsiri, S. Mangmool, K. Wongsariya, and D. Ochaikul, "Characteristics and upregulation of antioxidant enzymes of kitchen mint and oolong tea kombucha beverages," (in English), *J. Food Biochem.,* Article vol. 45, no. 1, p. 14, Jan 2021, Art no. e13574, doi: 10.1111/jfbc.13574.

[4] T. Tanaka and Y. Matsuo, "Production Mechanisms of Black Tea Polyphenols," (in English), *Chem. Pharm. Bull.,* Review vol. 68, no. 12, pp. 1131-1142, Dec 2020, doi: 10.1248/cpb.c20-00295.

[5] W. Jian, Z. Xianyin, and D. ShiPing, "Identification and grading of tea using computer vision," (in English), *Applied Engineering in Agriculture,* Article vol. 26, no. 4, pp. 639-645, Jul 2010. [Online]. Available: <Go to ISI>://WOS:000281451600011.

[6] X. J. Yu, K. S. Liu, Y. He, and D. Wu, "Color and Texture Classification of Green Tea Using Least Squares Support Vector Machine (LSSVM)," in *Components, Packaging and Manufacturing Technology*, vol. 460-461, Y. W. Wu Ed., (Key Engineering Materials. Stafa-Zurich: Trans Tech Publications Ltd, 2011, pp. 774-779.

[7] Y. D. Zhang, K. Muhammad, and C. Tang, "Twelve-layer deep convolutional neural network with stochastic pooling for tea category classification on GPU platform," *Multimedia Tools & Applications,* 2018.

[8] L. H. Lin, C. H. Li, S. Yang, S. Z. Li, and Y. Wei, "Automated classification of Wuyi rock tealeaves based on support vectormachine," *Concurrency Practice & Experience,* vol. 31, no. 23, pp. e4519.1-e4519.9, 2019.

[9] J. Yang, "Identification of green, Oolong and black teas in China via wavelet packet entropy and fuzzy support vector machine," *Entropy,* Article vol. 17, no. 10, pp. 6663-6682, 2015, doi: 10.3390/e17106663.

[10] G. Ren, J. Ning, and Z. Zhang, "Multi-variable selection strategy based on near-infrared spectra for the rapid description of dianhong black tea quality," *Spectrochimica Acta Part A Molecular & Biomolecular Spectroscopy,* vol. 245, 2020.

[11] X. Wu, "Tea category identification based on optimal wavelet entropy and weighted k-Nearest Neighbors algorithm," *Multimedia Tools and Applications,* journal article vol. 77, no. 3, pp. 3745-3759, 2018, doi: 10.1007/s11042-016-3931-z.

[12] C. Cattani and R. Rao, "Tea Category Identification Using a Novel Fractional Fourier Entropy and Jaya Algorithm," *Entropy,* vol. 18, no. 3, 2016, Art no. 77, doi: 10.3390/e18030077.

[13] A. J. Liu, "Tea Category Identification using Computer Vision and Generalized Eigenvalue Proximal SVM," (in English), *Fundamenta Informaticae,* Article vol. 151, no. 1-4, pp. 325-339, 2017, doi: 10.3233/fi-2017-1495.

[14] Y. Chen and X. Chen, "Tea Leaves Identification Based on Gray-Level Co-occurrence Matrix and K-Nearest Neighbors Algorithm," *AIP Conference Proceedings,* vol. 2073, 2019, Art no. 020084.

[15] J. Ajayakumar *et al.*, "Exploring convolutional neural networks and spatial video for on-the-ground mapping in informal settlements," (in English), *Int. J. Health Geogr.,* Article vol. 20, no. 1, p. 17, Dec 2021, Art no. 5, doi: 10.1186/s12942-021-00259-z.

[16] B. McIlwaine and M. R. Casado, "JellyNet: The convolutional neural network jellyfish bloom detector," (in English), *Int. J. Appl. Earth Obs. Geoinf.,* Article vol. 97, p. 13, May 2021, Art no. 102279, doi: 10.1016/j.jag.2020.102279.

[17] Y.-D. Lv, "Alcoholism detection by data augmentation and convolutional neural network with stochastic pooling," *Journal of Medical Systems,* vol. 42, no. 1, 2018, Art no. 2.

[18] C. Pan, "Abnormal breast identification by nine-layer convolutional neural network with parametric rectified linear unit and rank-based stochastic pooling," *Journal of Computational Science,* vol. 27, pp. 57-68, 2018, doi: https://doi.org/10.1016/j.jocs.2018.05.005.

[19] C. Huang, "Multiple Sclerosis Identification by 14-Layer Convolutional Neural Network With Batch Normalization, Dropout, and Stochastic Pooling," (in English), *Frontiers in Neuroscience,* Original Research vol. 12, 2018-November-08 2018, Art no. 818, doi: 10.3389/fnins.2018.00818.

[20] A. M. Hamer, D. M. Simms, and T. W. Waine, "Replacing human interpretation of agricultural land in Afghanistan with a deep convolutional neural network," (in English), *International Journal of Remote Sensing,* Article vol. 42, no. 8, pp. 3017-3038, Apr 2021, doi: 10.1080/01431161.2020.1864059.

[21] I. Urbaniak and M. Wolter, "Quality assessment of compressed and resized medical images based on pattern recognition using a convolutional neural network," (in English), *Communications in Nonlinear Science and Numerical Simulation,* Article vol. 95, p. 13, Apr 2021, Art no. 105582, doi: 10.1016/j.cnsns.2020.105582.

[22] T. N. Nguyen, A. S. Podkowa, T. H. Park, R. J. Miller, M. N. Do, and M. L. Oelze, "USE OF A CONVOLUTIONAL NEURAL NETWORK AND QUANTITATIVE ULTRASOUND FOR DIAGNOSIS OF FATTY LIVER," (in English), *Ultrasound Med. Biol.,* Article vol. 47, no. 3, pp. 556-568, Mar 2021, doi: 10.1016/j.ultrasmedbio.2020.10.025.

[23] K. Muhammad, "Image based fruit category classification by 13-layer deep convolutional neural network and data augmentation," *Multimedia Tools and Applications,* vol. 78, no. 3, pp. 3613-3632, 2019, doi: 10.1007/s11042-017-5243-3.

[24] S. Xie, "Alcoholism Identification Based on an AlexNet Transfer Learning Model," (in English), *Frontiers in Psychiatry,* Original Research vol. 10, 2019-April-11 2019, Art no. 205, doi: 10.3389/fpsyt.2019.00205.

[25] J. Kakarla, B. V. Isunuri, K. S. Doppalapudi, and K. S. R. Bylapudi, "Three-class classification of brain magnetic resonance images using average-pooling convolutional neural network," *International Journal of Imaging Systems and Technology,* p. 10doi: 10.1002/ima.22554.

[26] K. Nomura, K. Fukushima, T. Matsumura, and S. Asai, "Burn-through prediction and weld depth estimation by deep learning model

monitoring the molten pool in gas metal arc welding with gap fluctuation," (in English), *Journal of Manufacturing Processes,* Article vol. 61, pp. 590-600, Jan 2021, doi: 10.1016/j.jmapro.2020.10.019.

[27] T. Vrzal, M. Maleckova, and J. Olsovska, "DeepRel: Deep learning-based gas chromatographic retention index predictor," (in English), *Anal. Chim. Acta,* Article vol. 1147, pp. 64-71, Feb 2021, doi: 10.1016/j.aca.2020.12.043.

[28] R. Arora, B. Raman, K. Nayyar, and R. Awasthi, "Automated skin lesion segmentation using attention-based deep convolutional neural network," (in English), *Biomedical Signal Processing and Control,* Article vol. 65, p. 10, Mar 2021, Art no. 102358, doi: 10.1016/j.bspc.2020.102358.

[29] S.-H. Wang, "Covid-19 Classification by FGCNet with Deep Feature Fusion from Graph Convolutional Network and Convolutional Neural Network," *Information Fusion,* vol. 67, pp. 208-229, 2020/10/09/ 2021, doi: 10.1016/j.inffus.2020.10.004.

[30] S.-H. Wang, "COVID-19 classification by CCSHNet with deep fusion using transfer learning and discriminant correlation analysis," *Information Fusion,* vol. 68, pp. 131-148, 2021, doi: 10.1016/j.inffus.2020.11.005.

[31] D. Kawahara, X. Y. Tang, C. K. Lee, Y. Nagata, and Y. Watanabe, "Predicting the Local Response of Metastatic Brain Tumor to Gamma Knife Radiosurgery by Radiomics With a Machine Learning Method," (in English), *Frontiers in Oncology,* Article vol. 10, p. 8, Jan 2021, Art no. 569461, doi: 10.3389/fonc.2020.569461.

[32] S. R. Dubey and S. Chakraborty, "Average biased ReLU based CNN descriptor for improved face retrieval," (in English), *Multimedia Tools and Applications,* Article; Early Access p. 26, 2021, doi: 10.1007/s11042-020-10269-x.

[33] M. Yamaguchi, G. Iwamoto, Y. Nishimura, H. Tamukoh, and T. Morie, "An Energy-Efficient Time-Domain Analog CMOS BinaryConnect Neural Network Processor Based on a Pulse-Width Modulation Approach," (in English), *IEEE Access,* Article vol. 9, pp. 2644-2654, 2021, doi: 10.1109/access.2020.3047619.

[34] D. Chicco, N. Totsch, and G. Jurman, "The Matthews correlation coefficient (MCC) is more reliable than balanced accuracy, bookmaker informedness, and markedness in two-class confusion matrix evaluation," (in English), *BioData Min.,* Article vol. 14, no. 1, p. 22, Dec 2021, Art no. 13, doi: 10.1186/s13040-021-00244-z.

[35] D. S. Guttery, "Improved Breast Cancer Classification Through Combining Graph Convolutional Network and Convolutional Neural Network," *Information Processing and Management,* vol. 58, 2, 2021, Art no. 102439.

[36] H. Akbari, M. T. Sadiq, and A. U. Rehman, "Classification of normal and depressed EEG signals based on centered correntropy of rhythms in empirical wavelet transform domain," (in English), *Health Inf. Sci. Syst.,* Article vol. 9, no. 1, p. 15, Dec 2021, Art no. 9, doi: 10.1007/s13755-021-00139-7.

[37] S. Banerjee and S. Monni, "An orthogonally equivariant estimator of the covariance matrix in high dimensions and for small sample sizes," (in English), *Journal of Statistical Planning and Inference,* Article vol. 213, pp. 16-32, Jul 2021, doi: 10.1016/j.jspi.2020.10.006.

[38] X. Jiang, S. C. Satapathy, L. Yang, S. H. Wang, and Y. D. Zhang, "A Survey on Artificial Intelligence in Chinese Sign Language Recognition," *Arabian Journal for Science and Engineering,* 2020.

[39] S. C. Satapathy, "A five-layer deep convolutional neural network with stochastic pooling for chest CT-based COVID-19 diagnosis," *Machine Vision and Applications,* vol. 32, 2021, Art no. 14.

[40] H. Lee, H. Jeong, G. Koo, J. Ban, and S. W. Kim, "Attention Recurrent Neural Network-Based Severity Estimation Method for Interturn Short-Circuit Fault in Permanent Magnet Synchronous Machines," (in English), *IEEE Transactions on Industrial Electronics,* Article vol. 68, no. 4, pp. 3445-3453, Apr 2021, doi: 10.1109/tie.2020.2978690.